

Study of a position-sensitive scintillator neutron detector^{*}

TANG Bin(唐彬)^{1;1)} SUN Zhi-Jia(孙志嘉)^{1;2;2)} ZHANG Qiang(张强)^{1;3} YANG Zhen(杨振)¹
XU Hong(许虹)¹ YANG Gui-An(杨桂安)¹ WANG Yan-Feng(王艳凤)¹
WU Chong(吴冲)³ CHEN Yuan-Bo(陈元柏)¹ YANG Lei(杨雷)³

¹ Institute of High Energy Physics, Chinese Academy of Sciences, Beijing 100049, China

² Dongguan University of Technology, Dongguan 523808, China

³ China University of Petroleum, Beijing 102249, China

Abstract: The investigation of a novel thermal neutron detector is developed to fulfill the requirements of the high intensity power diffractometer (HIPD) at the Chinese Spallation Neutron Source (CSNS). It consists of two layers of ⁶LiF/ZnS(Ag) scintillators, two layers of crossed WLSF arrays, several multi-anode photo multiplier tubes (MA-PMT), and the matching readout electronics. The neutron detection efficiency of the scintillators, the light transportation ability of the WLSF, and the spatial linearity of the readout electronics are measured and discussed in this paper. It shows that the sandwich structure and the compact readout electronics could fulfill the needs of the HIPD. A prototype with a 10 cm×10 cm sensitive area has been constructed to further study the characteristics of the neutron scintillator detector.

Key words: ⁶LiF/ZnS(Ag) scintillator, neutron detector, wavelength shifting fiber, detection efficiency

PACS: 29.30.Hs, 29.40.-n, 29.40.Gx **DOI:** 10.1088/1674-1137/36/11/009

1 Introduction

Thermal neutron scattering techniques play an important role in the diffraction experiments performed to determine the molecular and crystal structures in biology, condensed state physics, and polymer chemistry, with which a high flux neutron source is required. High-intensity pulsed neutron sources have made great progress in the world in recent years [1, 2]. The Chinese Spallation Neutron Source (CSNS) is under construction in Guangdong Province. Three neutron spectrometers will be installed during the first phase of the project. The high intensity power diffractometer (HIPD) is one of the three day-one neutron instruments for CSNS. It is designed mainly for the determination of the crystallographic and magnetic structures with high intensity and good resolution. The detector is one of the key pieces of equipment and has a big influence on the

performance of the instrument, especially the position resolution.

The ³He neutron detector is ideal for many neutron spectrometers. However, due to the shortage of ³He gas and the rapidly increasing price, seeking new neutron detectors to replace the ³He neutron detector is urgent. ZnS(Ag) scintillator doped with ⁶LiF is a good candidate for use in thermal neutron detectors [3–5]. The advantages of a scintillator detector, including high efficiency, high resolution, low n/γ rejection ratio, real-time detecting, and so on, make it suitable for our HIPD instrument. We have adopted the simple bank concept, and planned 13.5 m² arrays for the high angle bank (150°) and 90° bank, and 0.8 m² for the low angle bank (15°). There are 116 detector modules to cover all banks. Table 1 gives the detailed main requirements for the detector modules in the HIPD [6].

The investigation of a novel thermal neutron de-

Received 7 February 2012, Revised 10 May 2012

* Supported by National Natural Science Foundation of China (11175257) and Key Laboratory of Neutron Detection and Electronics of Dongguan Municipality

1) E-mail: tangb@ihep.ac.cn

2) E-mail: Sunzj@ihep.ac.cn

©2012 Chinese Physical Society and the Institute of High Energy Physics of the Chinese Academy of Sciences and the Institute of Modern Physics of the Chinese Academy of Sciences and IOP Publishing Ltd

detector using a ${}^6\text{LiF}/\text{ZnS}(\text{Ag})$ scintillator and wavelength-shifting fibers (WLSFs) is reported in this paper. The ${}^6\text{LiF}/\text{ZnS}(\text{Ag})$ scintillator is chosen as the neutron convertor. The WLSFs are used to collect the luminescent light generated in the scintillator. Compact readout electronics have been designed to reduce the electronic channels and the cost. The neutron detection efficiency of the scintillators, the light transportation ability of the WLSF, and the spatial linearity of the readout electronics are measured to support the detector design. A prototype with a 10 cm×10 cm sensitive area has been constructed to further study the characteristics of the neutron scintillator detector.

Table 1. The main parameters of the detector modules for the HIPD.

main technical parameters	parameter index
active area	220 mm×480 mm
neutron detection efficiency	> 40%@1.8 Å
spatial resolution	< 5 mm×50 mm
count rate per module	> 30 kHz

2 The detector design

Figure 1(a) shows the schematic layout of the

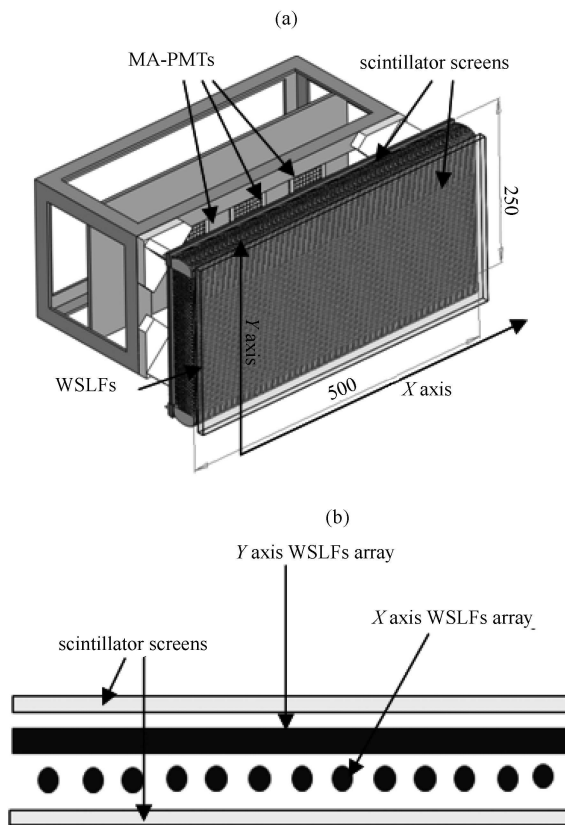


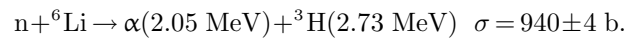
Fig. 1. (a) Schematic layout of the scintillator detector; (b) profile map of the head of the scintillator detector.

neutron scintillator detector. It consists of two layers of ${}^6\text{LiF}/\text{ZnS}(\text{Ag})$ scintillator, two layers of crossed WLSF arrays, several multi-anode photo multiplier tubes (MA-PMT), and the matching readout electronics. Fig. 1(b) shows a profile map of the head of the detector. Two layers of ${}^6\text{LiF}/\text{ZnS}(\text{Ag})$ scintillator are placed at the front and back of two crossed WLSF arrays. For the double-layer sandwich structure, the thermal neutron detection efficiency could reach more than 40% when an appropriate scintillator is chosen.

3 The experimental measurements and discussion

3.1 The scintillator

The ${}^6\text{LiF}/\text{ZnS}(\text{Ag})$ scintillator is a good candidate for the large-area scintillator screens in the HIPD. It has a large light yield and a moderate first decay component of 200 ns. Neutrons are detected by the following neutron reaction:



The thermal neutron detection efficiency of the detector module is required to be more than 40%. It is decided by the neutron-convertor efficiency and the light number which could be transmitted to the MA-PMT to trigger the electronics.

The screens commercially available at present have different thicknesses and ${}^6\text{LiF}/\text{ZnS}(\text{Ag})$ ratio by weight. The thickness of 400 μm is considered as an appropriate value for the outgoing scintillation light and for the mechanical strength. We have obtained three ${}^6\text{LiF}/\text{ZnS}(\text{Ag})$ samples with different amounts of ${}^6\text{LiF}$. The detection efficiency and the light yield from the surface of the scintillator are measured and discussed here.

3.1.1 The experimental setup

The neutron detection efficiencies of three scintillators are measured on a neutron test platform with a ${}^{252}\text{Cf}$ neutron source. The neutron source is placed in a shielding barrel with a $\Phi 10$ cm collimating aperture. The neutrons with an average energy of 2.13 MeV emitting from the ${}^{252}\text{Cf}$ source are moderated by a polythene block of 10 cm in thickness. A stander high pressure ${}^3\text{He}$ MWPC is used to calibrate the exit neutron number before the measurements. The scintillator is coupled by air to the PMT XP2020, and is placed in a dark box. The neutron count rates and the charge distributions of the neutron pulses are obtained through the electronics and the ADC system.

3.1.2 The neutron signal

The count rate of the detector module is required to be more than 30 kHz. The neutron signal we obtained from the ${}^6\text{LiF}/\text{ZnS}(\text{Ag})$ scintillator is shown in Fig. 2. The pulse is about 300 ns wide with the rising time less than 20 ns. So the requirement of the count rate is easy to fulfill. Because of the light attenuation and the different positions of the nuclear reactions inside the scintillator, the amplitudes of the neutron pluses are between 100–300 mV.

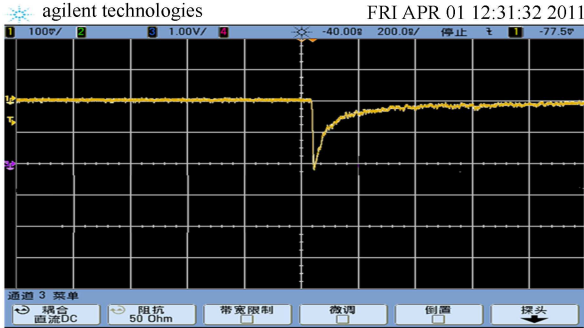


Fig. 2. A typical neutron signal from the oscilloscope.

3.1.3 The detection efficiency

Table 2 shows the characteristics of three ${}^6\text{LiF}/\text{ZnS}(\text{Ag})$ samples we obtained. The background, which may come from cosmic rays, is measured before the experiment. It is only a magnitude of 10^{-3} per second. The backgrounds of the gamma ray can be reduced rapidly by the discriminator of the electronics. Even the high energy gamma ray can be discriminated from the neutron signal by charge distribution (see Fig. 3). Compared with the measurement result of the stander high pressure ${}^3\text{He}$ MWPC, we have estimated the neutron detection efficiency of three ${}^6\text{LiF}/\text{ZnS}(\text{Ag})$ scintillator samples.

There is clearly an increase in neutron counting rate as the ${}^6\text{LiF}$ ratio goes from 1:4 to 1:2. Because of the light absorption in ${}^6\text{LiF}/\text{ZnS}(\text{Ag})$ scintillator and the different energy distribution of the moderated neutron in our experiment, the detection efficiencies we obtained are less than the reference detection effi-

ciency from the manufacturers. Considering the statistical error, the deviations of the neutron detection efficiencies between three samples and the references are appropriate.

By increasing the neutron-converter material ${}^6\text{LiF}$, and by optimizing the manufacturing technologies to reduce the light absorption of the scintillator, the detection efficiency can be improved. The BC-704# with the highest ${}^6\text{LiF}$ ratio did not obtain the best detection efficiency as expected. A reasonable explanation is the better manufacture technologies used at the Eljen Technology factory. It reduced the light absorption in ${}^6\text{LiF}/\text{ZnS}(\text{Ag})$ scintillator. Another reason may be that further increase of the ${}^6\text{LiF}$ will reduce the light transparency of the scintillator. A similar result can be found in ${}^{10}\text{B}_2\text{O}_3/\text{ZnS}(\text{Ag})$ [9].

3.1.4 The light yield

The light yield number from the surface of the samples could be calculated through measurement of the single photoelectron peak of the PMT XP2020. Fig. 3 shows the charge distributions of the neutron signals for three ${}^6\text{LiF}/\text{ZnS}(\text{Ag})$ samples. The number of primary luminescent light of the ${}^6\text{LiF}/\text{ZnS}(\text{Ag})$ scintillator could reach up to 1.6×10^5 photons per neutron. Because of the light absorption in ${}^6\text{LiF}/\text{ZnS}(\text{Ag})$, the light yields from the surfaces of three scintillators BC-704, BC-704# and EJ-426 are about 5.8×10^3 , 6.1×10^3 and 8.0×10^3 , respectively. The differences for the light yield among these samples are mainly caused by the different manufacturing technologies corresponding to different light absorption values.

3.2 The WLSF

The BC-91A WLSF is chosen to collect the scintillation light, with which the light is transported to the MA-PMTs by wavelength shifting. The sketch of a double-clad fiber including two layers of cladding provides highly efficient reflective surfaces, and a wavelength-shifting core for the re-emitted light [10]. It has been reported that the light yield increases

Table 2. The characteristics of three scintillator samples.

type	BC-704 [7]	BC-704# [7]	EJ-426 [8]
${}^6\text{LiF}:\text{ZnS}$ weight ratio	1:4	1:2	1:3
thickness/ μm	400	400	400
size	25 mm \times 25 mm	25 mm \times 25 mm	25 mm \times 25 mm
manufacturer	Saint-Gobain	Saint-Gobain	Eljen technology
counting rate/(n/s \cdot cm 2)	0.53 \pm 0.04	0.69 \pm 0.04	0.74 \pm 0.03
neutron detection efficiency (%)	23.2 \pm 7.5	30.2 \pm 5.8	32.4 \pm 4.1
reference detection efficiency (%)	26.4	—	36.3

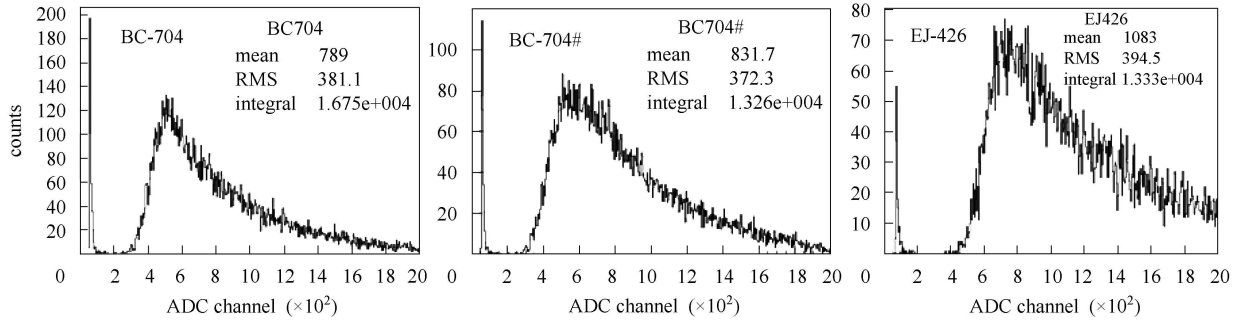


Fig. 3. The charge distribution of neutron signals for three ${}^6\text{LiF/ZnS(Ag)}$ samples.

almost linearly with the diameter of WLS fiber [11]. The fiber with a diameter of 1.0 mm is chosen as a reasonable compromise between the light output and the fiber flexibility. They are then polished and bent to be coupled to the MA-PMTs.

3.2.1 Layout of the arrays

In order to get the position resolution of better than $5\text{ mm}\times 50\text{ mm}$, the layout of the WLSFs arrays should be designed meticulously. For the detector module, there are 240 WLSFs in one dimension (X axis), and 110 WLSFs for another (Y axis). The X axis of WLSFs spans 480 mm in length, and the Y axis of WLSFs spans 220 mm in width, respectively. The WLSFs are all placed with a 2 mm center-to-center space. To balance the pixel size and the electronics channels, 2 adjacent fibers of the X axis are put together, and 10 adjacent fibers of the Y axis are put together. There are 120 clusters in the X axis, and 11 clusters in the Y axis. So the pixel size of the module could reach $4\text{ mm}\times 20\text{ mm}$, which is much less than the requirement of the HIPD. There are 3 MA-PMTs to collect the light from the WLSFs. Each cluster of the WLSFs is coupled to one working unit of the MA-PMTs. 120 clusters in the X axis are coupled to two MA-PMTs with 128 working units in all. 11 clusters in the Y axis are coupled to another MA-PMT.

3.2.2 The light transportation ability

We define a parameter C_{collect} to present the light transportation ability of the WLSF. It could be measured by experiment.

$$C_{\text{collect}} = N_{\text{green}}/N_{\text{blue}}, \quad (1)$$

where N_{blue} is the number of blue light irradiating on the WLSF, N_{green} is the green light number of the WLSF collected by the PMT. By using a calibrated PMT and an exactitude collimator, the light transportation ability of WLSFs C_{collect} we obtained is about 6%. The C_{collect} offered by the manufactory

is larger than 5.6%. This value fits our experimental result well.

We have also measured the bending loss of the WLSF with a different radius. With increasing the bending radius, the bending loss is reduced exponentially. To balance the light output and the compact structure of the detector module, the radius of 20 mm with 6.3% bending loss is chosen as a reasonable compromise.

3.3 MA-PMT

The H8500 is a 12-stage, square 25 cm^2 flat panel multi-anode photomultiplier with a matrix of 8×8 anodes for charge collection and position sensing. The tube can be supplied with a high voltage in the range from -700 to -1100V giving a gain that spans from 5×10^4 to 2×10^6 . In our scintillator detector, the 64 working units of each H8500 are coupled with several WLSFs to get the $4\text{ mm}\times 20\text{ mm}$ pixel. The compact discretized positioning circuit (DPC) [12] was built by us to reduce the channel number and the cost of the readout electronics.

The discretized positioning circuit (DPC) consists of an array of resistors that divide the charge between low impedance. Fig. 4 shows the DPC schematic circuit diagram. It splits the charge proportional to its Cartesian coordinates. This charge is collected by 4 charge-sensitive preamplifiers named A , B , C , and D . The X and Y position can be determined by:

$$\begin{aligned} X_{\text{position}} &= (A+B)/(A+B+C+D) \\ Y_{\text{position}} &= (A+D)/(A+B+C+D). \end{aligned} \quad (2)$$

The signal from the cathode Dy12 of H8500 is used as the trigger of the electronics. The amplitude of this signal is also used to discriminate the multi-hit events. By using the matched equal valued resistors, the DPC readout electronics could get an excellent spatial linearity. The spatial response measurement of the H8500 and the DPC readout electronics is shown in Fig. 5. By changing the position of the

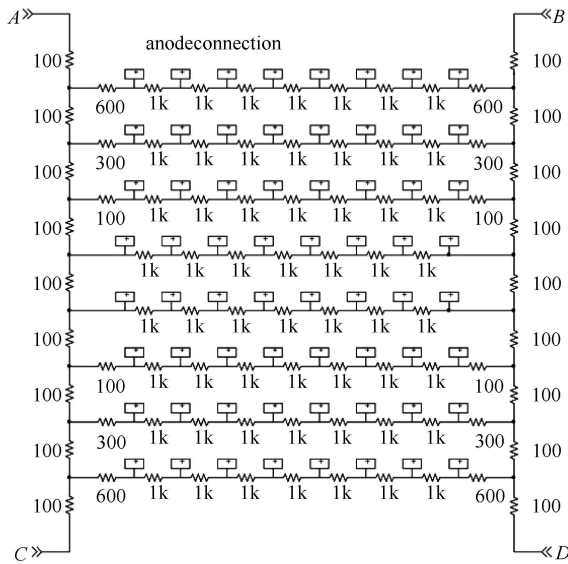


Fig. 4. The DPC schematic circuit diagram.

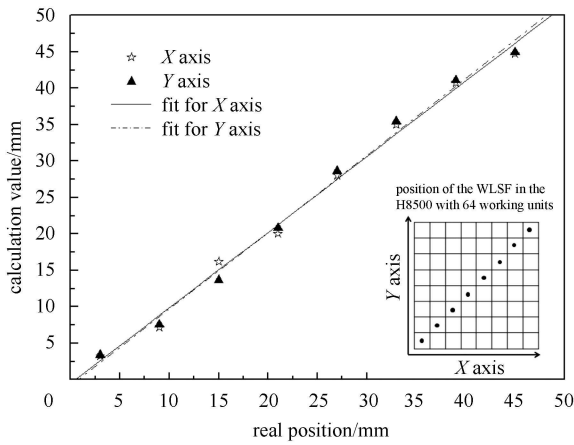


Fig. 5. The linearity measurement results.

WLSF, the spatial response of H8500 and the DPC readout electronics is obtained. The spatial linearity of the DPC readout electronics is better than 95% for the *X* axis and *Y* axis.

4 The detector prototype

In order to further study the characteristics of the scintillator neutron detector, a prototype with a 10 cm×10 cm sensitive area has been constructed. Two WLSF-arrays are sandwiched by two ⁶LiF/ZnS(Ag) scintillators. Each WLSF-array has 64 1-mm-diameter fibers, with 1.5 mm center-to-center space. The fibers are mounted in slotted brackets to establish the space. Soft silicone rubber gaskets are used at the end of the fibers to hold them in place. This structure defines the 1.5 mm×1.5 mm pixel size, which is much less than the requirement of the HIPD. The goal of this is to obtain the minimum position resolution of the scintillator detector with wavelength shifting fiber structure. The gap from the scintillator screen to the WLSFs array is 1 mm. Two H8500 MA-PMTs with DPC readout electronics are used to decide the position of the incident neutron.

Figure 6 shows the picture of the prototype: (a) is the whole view of the prototype, and (b) is the double WLSF-arrays of our prototype. The entire prototype assembly is about 15 cm×15 cm×33 cm. The box is light tight during operation, but it is easy to change the front plate for scintillator assembly. The back is also easily accessible for work on the fiber assembly and the MA-PMTs. This prototype will be tested by using a ²⁵²Cf neutron source in the near future.

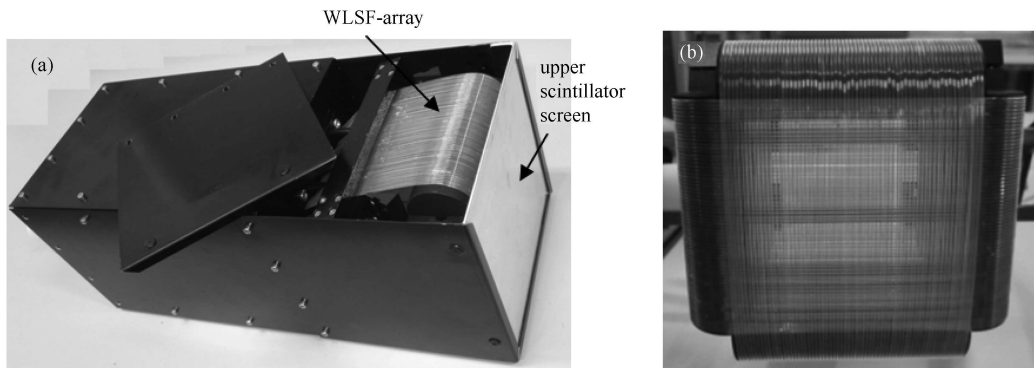


Fig. 6. The picture of the prototype: (a) the whole view of the prototype; (b) the double WLSF-arrays assigned on the prototype.

5 Conclusion and prospects

A position-sensitive scintillator neutron detector using wavelength-shifting fibers has been designed for the HIPD. The neutron detection efficiency of the ${}^6\text{LiF}/\text{ZnS}(\text{Ag})$ scintillators, the transportation characteristics of the BC-91A WLSF, and the spatial linearity of the MA-PMT H8500 with the DPC readout electronics are measured to support the design of the neutron detector system.

Because of the better neutron detection efficiency of 32.4% and the larger light yield of 8.0×10^3 /neutron, the EJ-426 sample could be a better scintillator candidate. For the double-layer sandwich structure, the neutron detection efficiency could reach up to 50% in theory when double EJ-426 scintillators are chosen. The neutron signal we obtained from the ${}^6\text{LiF}/\text{ZnS}(\text{Ag})$ scintillator is fast enough to allow the electronics to process in 1 μs . So the count rate of more than 30 kHz is easy to obtain. The light transportation ability for the WLSF is about 6%. The light number transported from the scintilla-

tor to the MA-PMT is about 400 per neutron. Taking the quantum efficiency of the H8500 for the green light into account, the light number can trigger the electronics successfully. With the good spatial linearity of the H8500 and the DPC readout electronics, the layout of the WLSF arrays with 2 mm and 4 mm center-to-center spaces in X axis and Y axis respectively could obtain position sensitivity of better than 5 mm \times 50 mm.

A prototype with a 10 cm \times 10 cm sensitive area has been constructed. The characteristics of the prototype are planned to be studied in the near future using other high intensity neutron sources.

Since the bending radius of the WLSFs is 2 cm, the active area of the prototype is only about 70% compared with its structural area. For the detector module with 250 mm \times 500 mm structural area, the ratio will increase by 84.5% when the bending radius of the WLSFs is still 2 cm. The package to minimize the dead area is also a high priority to the 6 m² detectors array. Further design efforts are required on the detector module for HIPD, especially on the large area WLSF-arrays.

References

- 1 Yamada Y, Watanabe N, Niimura N et al. *Physica B*, 1998, **42**: 241
- 2 WEI Jie. *Modern Physics*, 2007, **06**: 22 (in Chinese)
- 3 Alex C. *Nucl. Instrum. Methods A*, 2005, **551**: 88
- 4 Rhodes N J, Wardle A G, Boram A J et al. *Nucl. Instrum. Methods A*, 1997, **392**: 315
- 5 Crow M L, Hodges J P, Cooper R G. *Nucl. Instrum. Methods A*, 2004, **529**: 287
- 6 HE Lun-Hua. CSNS High Intensity Powder Diffractometer. In: CSNS International Advisory Committee Review Meeting Beijing, China 2011. 923
- 7 <http://www.eljentechnology.com/index.php/joomla-overview/neutron-detectors/113-ej-426>
- 8 <http://www.detectors.saint-gobain.com/.../Organics-Brochure.pdf>
- 9 Kojima T, Katagiri M, Tsutsui N et al. *Nucl. Instrum. Methods A*, 2004, **529**: 325
- 10 <http://www.detectors.saint-gobain.com/fibers.aspx>
- 11 YAO Shun, PANG Xiao-Lin, DAI Jing-Jing et al. *Acta Optica Sinica.*, 2011, **31**: 44 (in Chinese)
- 12 Olcott P D, Talcott J A, Levin C S et al. *IEEE Trans. Nucl. Sci.*, 2005, **52**: 21